J Nanostruct 15(4): 2353-2363, Autumn 2025

RESEARCH PAPER

Enhancing the Performance of Solar Thermal Collectors Using Nanocomposite (Nitrogen-Doped Carbon Quantum Dots Combined with Zinc Titanate) Extracted from *Malva Sylvestris*

Ali Al-Jubainawi [1] *, Noor Sabah Khadim [2], Ali Jasim Mohammed [1]

[1] *Department of Mechanical Engineering, College of Engineering, University of Misan, Maysan, Iraq*

[2] *Department of Pharmaceutical Chemistry, College of Pharmacy, University of Misan, Maysan, Iraq*

ARTICLE INFO

Article History:
Received 14 August 2025
Accepted 28 September 2025
Published 01 October 2025

Keywords:
Absorption of visible light
Efficiency of energy conversion
Malva sylvestris
N-CQDs
Solar thermal collector
$Zn_2Ti_3O_8$

ABSTRACT

Improving efficiency of solar thermal collectors using the nitrogen-doped carbon quantum dots/$Zn_2Ti_3O_8$ (N-CQDs/ZTO) nanocomposites extracted from Malva sylvestris is promising for enhancing the thermal sustainability. This nanocomposite is considered a natural source of carbon and nitrogen used as a component in a spectrally selective solar absorber coating. The N-CQDs/ZTO, which made them better at absorbing visible spectrum and moving charge carriers. Transmission electron microscopy (TEM) confirmed the consistent distribution of N-CQDs on the $Zn_2Ti_3O_8$ surface. Diffuse reflectance spectroscopy (DRS) showed a significant red shift and a smaller band gap (2.73 eV) when compared to pristine $Zn_2Ti_3O_8$ (3.36 eV). Photoluminescence (PL) studies showed better electron-hole separation efficiency. The N-CQDs/ZTO nanocomposite demonstrated remarkable photocatalytic degradation capacity for methylene blue (MB) after 120 minutes of exposure to visible light, achieving a 91.7% elimination rate. Throughout a sequence of five cycles, the examination on the solution pH, catalyst loading and oxidant concentration reveals that the thermal performance of solar collector would be more active and stable. The enhancement of the solar thermal collector with nanocomposite showed that it could work better as a photocatalyst, which means it could be used in hybrid solar thermal–photocatalytic systems. The N-CQDs/ZTO nanocomposite is a good candidate for use in solar thermal collectors and other renewable energy conversion systems because its optical and thermal properties work together to improve the overall efficiency of solar energy use.

How to cite this article
Al-Jubainawi A., Khadim N., Mohammed A. Enhancing the Performance of Solar Thermal Collectors Using Nanocomposite (Nitrogen-Doped Carbon Quantum Dots Combined with Zinc Titanate) Extracted from Malva Sylvestris. J Nanostruct, 2025; 15(4):2353-2363. DOI: 10.22052/JNS.2025.04.073

INTRODUCTION

The growing global requirement for clean and sustainable energy has paid many attention into the solar technology that can convert sunlight into useful forms of energy [1, 2]. Solar thermal and photocatalytic systems are technologies that can convert sunlight into heat, electricity, or even chemicals with less impact on the eco-system. To enhance the performance of these systems in the wide field of renewable energy [3], materials

* *Corresponding Author Email: alihussein.mcm@uomisan.edu.iq*

This work is licensed under the Creative Commons Attribution 4.0 International License.
To view a copy of this license, visit http://creativecommons.org/licenses/by/4.0/.

with high ability for absorbing and converting solar energy to heat, have been used. In recent years, solar thermal collectors (STCs) have been recognized as sustainable technology collecting solar and converting into heat that can be used for domestic and industrial applications [4]. The new technology represented by coating STCs with nanocomposite materials to perform both photothermal conversion and photocatalysis at the same time is a new method for maximizing solar collecting. These nanocomposites with two functions can improve the efficiency of solar thermal systems by increasing the thermal conductivity, light absorption, and stability of collector fluids.

Carbon quantum dots (CQDs) are defined as unique spherical carbon nanoparticles that are less than 10 nm in size [5, 6]. They get a lot of attention because their unique optical and electronic properties make them good candidates for solar energy harvesting, photothermal conversion, and photocatalytic enhancement. CQDs have been effectively employed in bio-imaging, chemiosensing, and biosensing [7, 8], and more recently, in solar-driven photocatalytic systems for energy and environmental applications. Adding nanostructured photocatalysts to solar thermal collector systems has become a popular way to make the most of sunlight. In these mixed systems, sunlight provides both photonic energy for photocatalytic excitation and thermal energy to speed up reactions. Materials demonstrating high visible-light absorption, elevated photothermal conversion efficiency, and structural durability at collector temperatures (60–120 °C) are thus imperative. [9, 10].

Recently, countless incidents of worldwide environmental crises—such as water and soil pollution— caused by destructive human activities have pushed the researchers to contemplate efficient ways to mitigate these problems [11-13]. Among the proposed method for getting rid the contaminants from soil and water, photocatalysis is of a great interest, and energy-efficient process [14, 15]. Photocatalysis utilizes solar or artificial light energy to degrade pollutants without leaving toxic by-products [15]. It is accomplished by utilizing a suitable semiconductor as a photocatalyst, which is activated by the light beam with energy equal or greater than the band gap of photocatalyst [16-18]. Although the photocatalytic degradation offers significant advantages over other treatment approaches, it still faces limitations due to the wide band gap of many photocatalysts [19]. Additionally, the photonic efficiency of the common photocatalyst materials is low, because of the fast recombination rate of photo-generated electrons and holes [20].

In this context, CQDs present a promising chance to enhance photocatalytic activity effectively [21]. CQDs with better electronic conductivity are expected to act as electron sinks, which will greatly improve charge separation and, in turn, increase the efficiency of photocatalytic and solar energy conversion [22-24]. For examples, Prabhakaran et al. studied photocatalytic degradation of methyl orange using CQDs/TiO_2 nanocomposite [25]. Najjar et al. prepared magnetically separable Fe_3O_4@CQDs photocatalyst for degradation of tetracycline [26]. Also, the photocatalytic degradation of sodium lignosulfonate has been reported using N-CQDs/$MgIn_2S_4$ composite [27].

The present work investigates a solar-responsive N-CQDs/$Zn_2Ti_3O_8$ nanocomposite designed as a multifunctional layer for STCs, capable of simultaneously capturing light and heat to enhance overall energy conversion efficiency. This research integrates solar-driven photocatalysis with thermal engineering, demonstrating how tailored nanocomposite structures could improve renewable and sustainable energy systems. Nitrogen-doped carbon quantum dots (N-CQDs) were produced by a straightforward hydrothermal procedure. A natural carbon source extracted from *Malva sylvestris* was used to synthesize N-CQDs. The N-CQDs were employed to enhance the visible-light sensitization of $Zn_2Ti_3O_8$ nanoparticles (ZTO), which were synthesized through the sol-gel reaction. First, the visible-light photoactivity of the N-CQDs/ZTO nanocomposites was verified by diffuse reflectance (DRS) and photoluminescence (PL) spectroscopy. Then, its photocatalytic activity was studied toward degradation of methylene blue (MB) under the visible light irradiation.

MATERIALS AND METHODS

Hydrothermal synthesis of nitrogen doped CQDs (N-CQDs)

First, 5.0 g of *Malva sylvestris* was put into 100 mL of deionized water and then heated to 90° C for 4h. The light yellow color solution was recovered by separation of solids using filter paper. 0.05 g of urea was added to the solution as a source of nitrogen. After that, the solution was poured into

(cc) BY

a Teflon-lined stainless steel autoclave and heating process was performed in an oven at 180° C for 6 h.

Sol-Gel synthesis of $Zn_2Ti_3O_8$ nanoparticles (ZTO)

The ZTO nanoparticles were synthesized using simple sol-gel reaction, as follows: first, 1.0 g of polyethylene glycol (PEG 600), as a capping agent, was dissolved in 50 mL of absolute ethanol. Then, 3.0 mmol tetrabutyl orthotitanate was added and stirred for 10 min. Next, 2.0 mmol of $Zn(NO_3)_2.6H_2O$ were added and stirred for 1 h. The solution was heated at a constant rate in an oven at 90 °C overnight to form a dried gel. The gel was calcined at 600 °C in a furnace for 5 h to obtain a pure crystalline powder.

Synthesis of N-CQDs/$Zn_2Ti_3O_8$ nanocomposite (N-CQDs/ZTO)

Specific amount of the as-synthesized ZTO nanoparticles were dispersed into 50 mL of N-CQDs solution and stirred for a day. Then, the nanoparticles were separated using centrifugation at 7000 rpm for 15 min. The separated nanoparticles were dries at 90° C overnight to prepared N-CQDs anchored on the ZTO nanoparticles—N-CQDs/ZTO nanocomposite.

Characterization

Crystalline phase of the ZTO, N-CQDs, and N-CQDs/ZTO samples was studied using X-ray diffraction pattern (XRD) by Philips X'pert Pro MPD (Cu Kα). Furrier transform infrared spectroscopy (FT-IR) was used to investigate the composition and chemical bonds of the N-CQDs and N-CQDs/ZTO samples. Morphology and structure of the N-CQDs and NCQDs/ZTO samples were studied using transmission electron microscope (TEM) (FEI Tecnai F20) and field emission scanning electron microscope (FESEM) (TESCAN Mira 3). Optical properties of the synthesized N-CQDs and N-CQDs/ZTO nanocomposite were studied using photoluminescence (PL) and diffuse reflectance (DRS) spectroscopy by Perkin Elmer LS 55 and JASCO UV/Vis spectrophotometer, respectively.

Photocatalytic experiments

The photocatalytic activity of the N-CQDs/ZTO nanocomposite was tested with respect to the pure ZTO nanoparticles for degradation of methylene blue (MB) under the visible light irradiation. An ordinary LED lamp (100 W) was used to the visible light initiation of the photocatalytic reaction. The reaction vessel was exposed to the light beams from the constant distance of 30 cm. First the reaction was carried out under darkness for 30 min to reach the adsorption/desorption equilibrium. Then, the reaction was followed under light illumination for 120 min, and the degradation level of MB was monitored at constant time interval (30 min). The absorption of the MB solution was determined using UV/Vis spectrophotometer at its maximum absorption wavelength (665 nm).

Solar-thermal simulation experiments

To simulate solar-collector conditions,

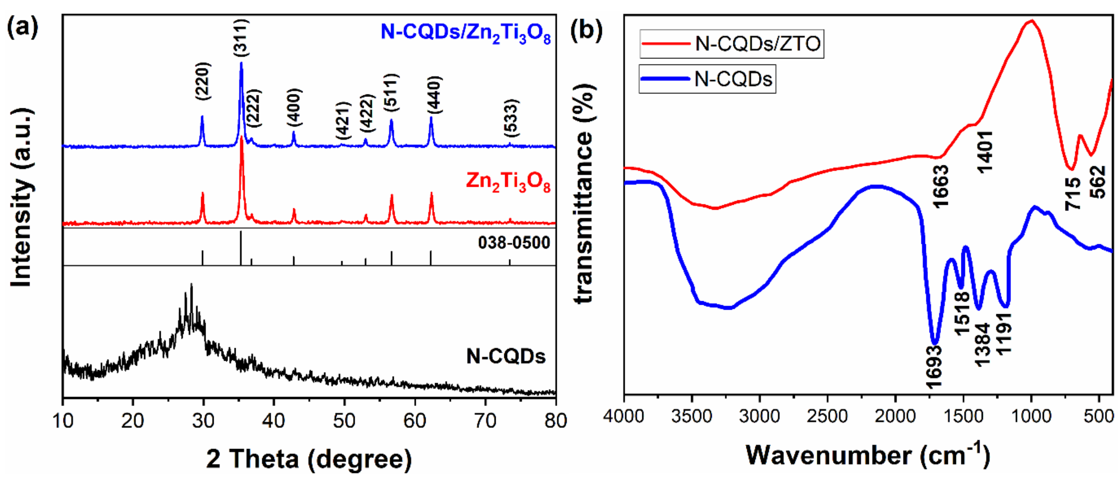

Fig. 1. XRD patterns (a) and FT-IR spectra (b) for the synthesized N-CQDs and NCQDs/ZTO.

photocatalytic reactions were performed under controlled temperatures (25–80 °C) using a thermostatic setup equipped with a simulated solar irradiance lamp (AM 1.5 G, 100 mW cm^{-2}). This configuration allowed evaluation of the synergistic influence of photonic and thermal energy on the degradation rate of methylene blue (MB). The temperature range corresponds to typical operational values of flat-plate solar collectors.

RESULTS AND DISCUSSION

Crystallinity and composition

Fig. 1a shows the diffraction patterns for the synthesized samples, including N-CQDs, ZTO nanoparticles and N-CQDs/ZTO nanocomposite. The observed reflections at 2Θ = 29.9°, 35.4°, 36.9°, 42.8°, 49.6°, 53.1°, 56.7°, 62.3°, 73.5° are matched with the cubic phase of zinc titanium oxide (JCPDS file no. 038-0500). As for the N-CQDs/ZTO nanocomposite, no prominent difference was observed in the diffraction pattern compared to the pure ZTO nanoparticles. This result is attributed to the attachment of the CQDs onto the surface of ZTO nanoparticles. In other words, the incorporation of N-CQDs does not alter the crystalline structure of the ZTO nanoparticles.

Additionally, the XRD pattern of the synthesized

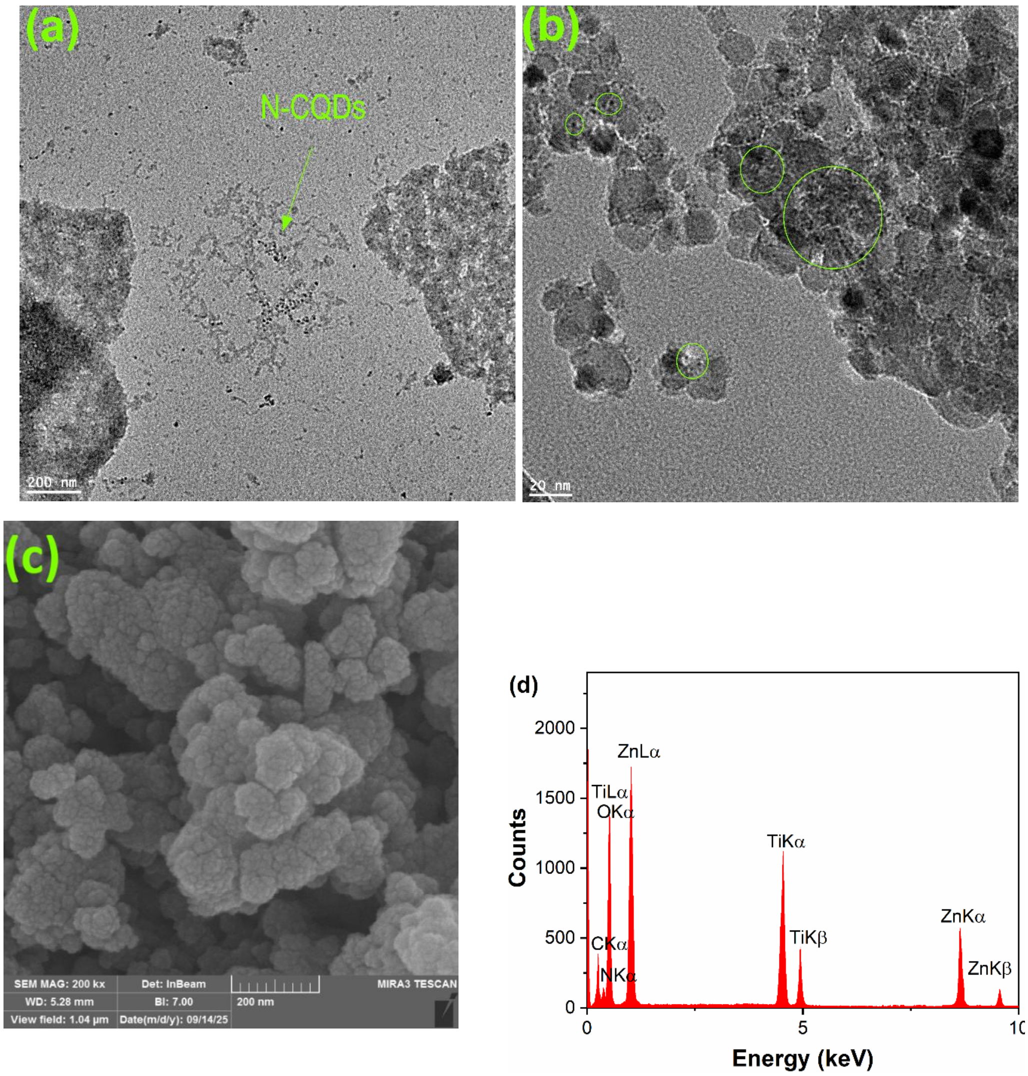

Fig. 2. TEM images for N-CQDs (a) and N-CQDs/ZTO nanocomposite (b), FESEM image (c), and EXD spectrum (d) for the N-CQDs/ZTO nanocomposite.

CC BY

N-CQDs, Fig. 1a, shows the broad peak around 2Ɵ = 26°, confirming the amorphous nature of the N-CQDs. The peak at 2Ɵ = 26° is attributed to the (002) diffraction plane of the hexagonal carbon (JCPDS file no 08-0415) [28, 29].

FT-IR spectra of the synthesized N-CQDs and N-CQDs/ZTO samples are provided in Fig. 1b. As seen from FT-IR spectrum of the N-CQDs, the broad absorption peak at 3400 cm^{-1} is assigned to the O-H bonds [30]. Also, the peaks at 1693, 1518, 1384, and 1191 cm^{-1} are related to the stretching vibration of C=O, C=C, C-N, C-O bonds [31, 32]. Besides, the presence of the N-CQDs on the surface of the ZTO nanoparticles was confirmed by FTIR analysis. The absorption peaks at 1663 cm^{-1} (C=O) and 1401cm^{-1} (C-N) are associated with the surface anchored N-CQDs. The bands at 715 and 562 min^{-1} are attributed to the Zn-O and Ti-O vibrations, respectively [33-35].

Morphology

The TEM image in Fig. 2a shows the dot-like nanoparticles for the synthesized N-CQDs. Also, Fig 2b reveals the black spots of the N-CQDs anchored on the surface of ZTO nanoparticles.

Moreover, the FESEM image of the synthesized N-CQDs/ZTO nanocomposite (Fig. 2c) shows the agglomerated particles consisting of fine spherical nanoparticles in the size range below 50 nm. Also, the EDX spectrum (Fig. 2d) represents the constituents of the nanocomposite with the relative amounts (wt%) of Ti (30.48%), Zn (26.78%), O (31.51%), C (9.41%), and N (1.82%).

Solar-thermal and thermo-mechanical stability

Fig. 3a shows the DRS spectra of the synthesized samples, disclosing that the visible-light absorption enhances with incorporation of the CQDs to the ZTO nanoparticles. Also, the narrowed band gap of the nanocomposite is highlighted in the inset to Fig. 3a. The determined band gap values of the samples are 2.73 and 3.36 eV for the N-CQDs/ZTO and pure ZTO samples, respectively. The decrease in the band gap of the nanocomposite is attributed to the formation of Ti-O-C bonds [36].

In addition, the efficiency of the charge separation was studied by the PL analysis, shown in Fig. 3b, exhibiting the decreased PL intensity by addition of the N-CQDs to the ZTO nanoparticles. The decrement in the PL intensity confirms the improved separation of the charges, which implies that the non-radiation relaxation is induced by incorporation of the N-CQDs to the ZTO nanoparticles [14]. The strong interfacial bonding between N-CQDs and $Zn_2Ti_3O_8$ provided excellent resistance to structural degradation under simulated solar-thermal cycling, confirming its suitability for long-term collector operation.

Photothermal Conversion Efficiency

The better ability of N-CQDs/ZTO to absorb visible light and separate charges is directly related to their better ability to convert light into heat. When light hits the nanocomposite suspension, non-radiative electron–hole recombination processes release heat in a small area, which causes the temperature to rise. This behavior indicates its

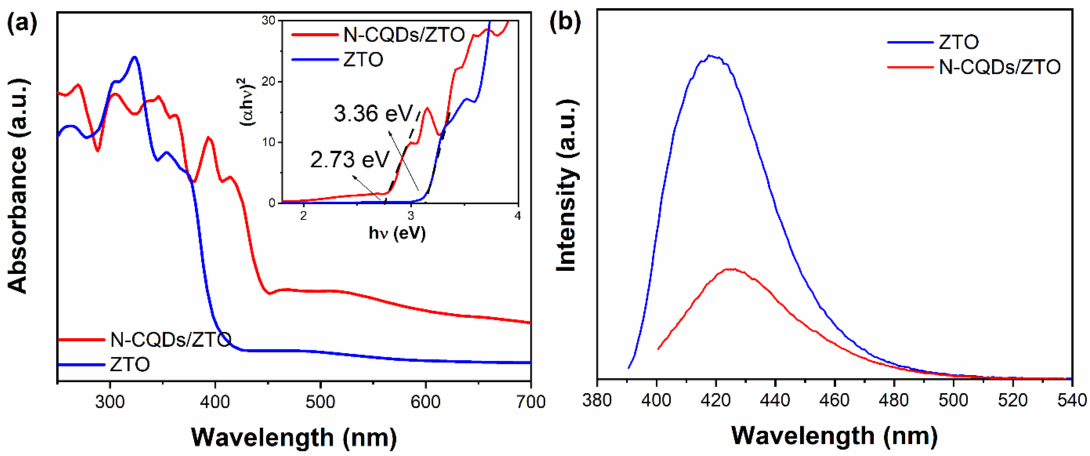

Fig. 3. DRS (a) and PL (b) spectra of N-CQDs/ZTO and ZTO. The inset to Fig. 3a shows Tauc plots for the synthesized samples that were made.

CC BY

strong potential as a photothermal medium for integration into solar thermal collector systems, where both heat generation and photocatalytic degradation can be simultaneously achieved.

Photocatalytic experiments

The photocatalytic activity of the synthesized N-CQDs/ZTO nanocomposite was investigated for the degradation of MB solution under the visible light irradiation. As shown in Fig. 4a, the photocatalytic degradation of the MB solution is about 91.7% using the N-CQDs/ZTO nanocomposite under visible light irradiation for 120 min, whereas the pure ZTO nanoparticles showed only 27.2% of the photocatalytic efficiency. Also, Fig. 4a shows that the degradation of MB solution is negligible under both no-light and no-catalyst conditions.

The kinetics of the photocatalytic reaction using the NCQDs/ZTO nanocomposite and ZTO nanoparticles are also depicted in Fig. 4b. As can be seen, by plotting $-Ln(C/C_0)$ versus the reaction time, it was confirmed that the photocatalytic degradation obeys from the first-order reaction kinetics—($-Ln(C/C_0) = KT$); C and C_0 are the concentration of MB solution after and before starting the photocatalytic reaction, K is the rate constant (min^{-1}), and T is the reaction time. The rate constant of the photocatalytic reaction was determined to be 0.603 and 0.071 min^{-1} using N-CQDs/ZTO nanocomposite and ZTO nanoparticles, respectively.

Effect of nanocomposite amount

Different amounts of the synthesized N-CQDs/ZTO nanocomposite were loaded into the MB solution and then the photocatalytic degradation was studied under constant irradiation time (120 min). Fig. 5 shows the photocatalytic degradation of the MB solution using the different amounts of the N-CQDs/ZTO nanocomposite. As seen, the optimum amount of the nanocomposite was found to be 0.04 g to achieve the highest photocatalytic efficiency. Further amounts of the nanocomposite led to the decrease in the photocatalytic level of the MB solution. The photocatalytic degradation of the MB solution was 87.2% and 59.5% using the 0.05 and 0.06 g of the N-CQDs/ZTO nanocomposite, respectively. This observation is attributed to the limited photo-excitation of the nanocomposite within the turbid solution, resulting from the impeded penetration of the light beams [37, 38]. The concentration-dependent response also reflects the material's photothermal sensitivity under visible-light exposure, where optimal nanocomposite concentration ensures efficient heat transfer within the collector medium

Effect of pH

The photocatalytic efficiency of the N-CQDs/ZTO nanocomposite was also assessed under different pH conditions. As illustrated in Fig. 6, the MB solution shows the higher degradation level in alkaline conditions compared to the acidic solutions. So that, the photocatalytic degradation of MB reached 94.6% and 98.1% under pH of 8 and 9, respectively. In contrast, the degradation efficiency of the MB solution decreased with decreasing the pH of MB solution. At pH of 5, the

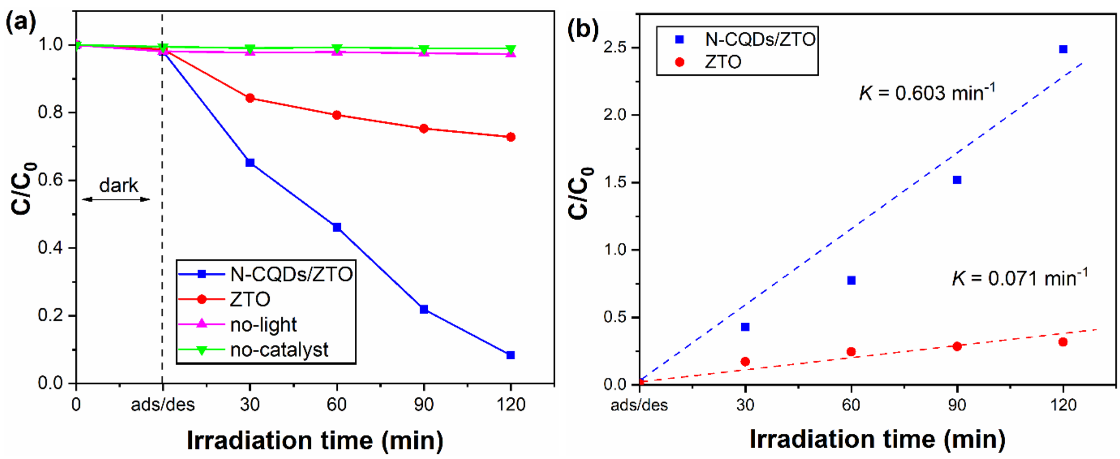

Fig. 4. Photocatalytic efficiency (a) and degradation kinetics curves (b) of N-CQDs/ZTO *vs*. pure ZTO.

CC BY

degradation of MB solution was 81.4%, which was further dropped to 61.2% at pH of 3.

These results revealed that the photocatalysis is strongly depended on pH of solution [39, 40]. Due to the fact that the photocatalytic reaction takes place mainly on the surface of photocatalyst, adsorption capacity of photocatalyst is an important determinant [41, 42]. The changing of the pH can alter the nature of charges on the surface of photocatalyst—as positive or negative charges—which in turn affects the adsorption capacity [40, 43]. Because the MB dye is the cationic in its nature [44], the negatively charged surface is more proper to have the enhanced adsorbed dye molecules on the surface of photocatalyst, thereby increasing the photocatalyst efficiency.

Effect of H_2O_2

The effect of H_2O_2, oxidant agent, on the photocatalytic degradation of MB was studied, which is provided in Fig. 7. As seen, the degradation level of MB solution increased to

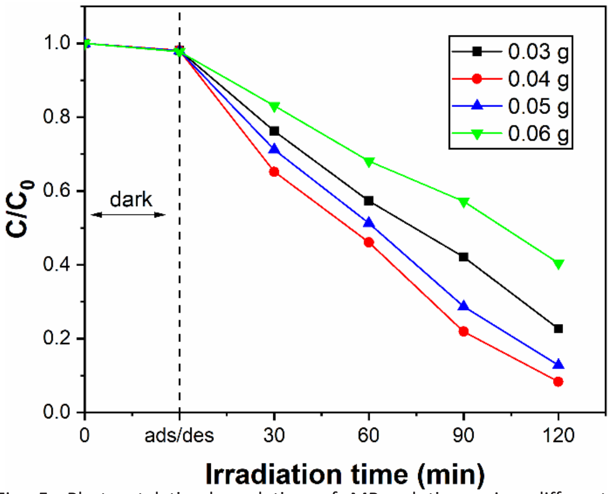

Fig. 5. Photocatalytic degradation of MB solution using different amounts of N-CQDs/ZTO nanocomposite.

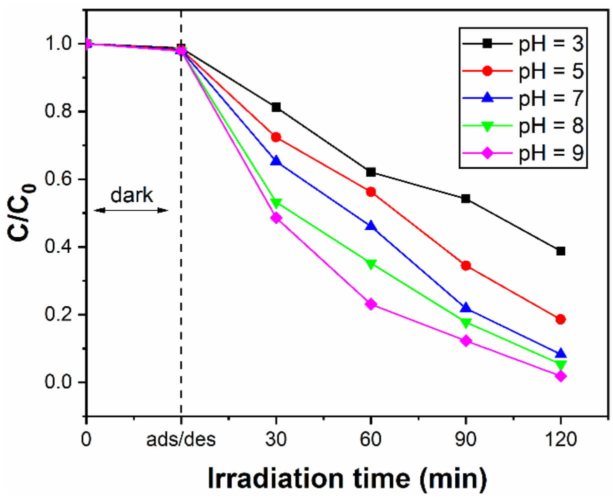

Fig. 6. Photocatalytic degradation of MB under different pH conditions.

cc BY

97.5% with addition 1.5 mL of H_2O_2 (1 mM). H_2O_2 can promote the release of hydroxyl radicals (•OH) by absorbing the photo-generated electrons, as following equation (Eq.1) [45]:

$$H_2O_2 \quad + \quad \text{photo} - \text{generated electrons} \quad \rightarrow \bullet OH \quad + \quad OH^-$$

However, more addition of the H_2O_2 led to the decrease in the photocatalytic degradation of MB solution, which is attributed to the loss of the •OH radicals by involving in the following reactions [46]:

$$H_2O_2 \quad + \quad \bullet OH \quad \rightarrow \quad H_2O \quad + \quad \bullet H_2O$$

$$H_2O \quad + \quad \bullet OH \quad \rightarrow \quad H_2O \quad + \quad O_2$$

Reusability experiments

The reusability is the key factor to efficiently utilize the photocatalysis for eliminating organic pollutants. The synthesized N-CQDs/ZTO nanocomposite was used to conduct 5 successive reaction cycles. To carry out the reusability tests, after each reaction, the nanocomposite particles were collected using centrifugation at 6000 rpm for 15 min. Then, collected particles were washed using ethanol/deionized water for three times and dried at 80 °C for 4 h.

Fig. 8 represents the reusability experiments for the degradation of MB solution using N-CQDs/ZTO nanocomposite over 5 reaction cycles. As seen, the synthesized nanocomposite exhibits the appreciable reusability. The loss of its photocatalytic efficiency is only 3.17% after 5 reaction cycles.

Photocatalytic mechanism

Fig. 9 represents the plausible mechanism for degradation of MB solution using the N-CQDs/ZTO nanocomposite. Upon illumination, the electrons in the nanocomposite are excited from the valence band (VB) to the conduction band (CB), leaving the positively charged holes in the VB. The photo-generated electrons are subsequently

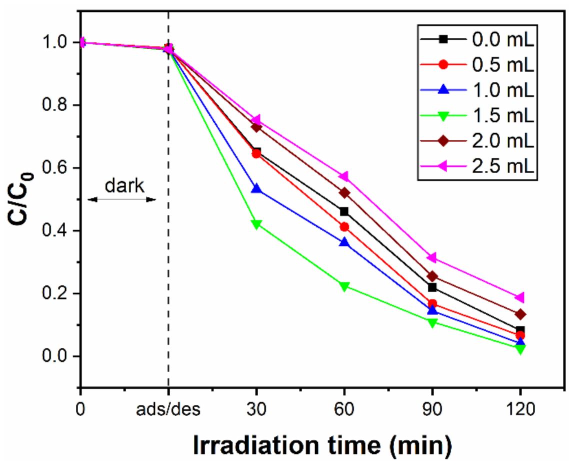

Fig. 7. Photocatalytic degradation of MB solution in the presence of different concentrations of H_2O_2.

Table 1. The degrading performance of photocatalysis in solar-thermal situations

Quantum efficiency apparent (%)	Constant of rate k (min^{-1})	Degradation (%) following 120 minutes	pH	H_2O_2 volume (mL)	Mass of the catalyst (g)	Temperature (°C)
15.2	0.603	91.7	7	1.0	0.04	25 °C (ambient)
17.6	0.645	95.8	7	1.0	0.04	50 °C
18.9	0.682	98.3	7	1.0	0.04	70 °C

CC BY

trapped by the surface-anchored N-CQDs, thereby suppressing their recombination with the holes. The holes contribute in the redox reactions leading to release •OH radicals, which then oxidize the MB molecule.

The proposed mechanism suggests that the absorbed photons are efficiently turned into thermal energy through non-radiative electron-hole recombination, in addition to photocatalytic degradation. This photothermal conversion effect can raise the temperature of the reaction medium a lot, which shows that the nanocomposite is good for use in solar thermal collectors, where both collecting heat and breaking down pollutants can happen at the same time.

Combining with solar thermal collectors

Nanostructured materials like N-CQDs/ZTO can work well as solar absorbers and heat transfer enhancers in solar thermal collectors. Because they can absorb a wide range of light and are very stable, they can be used as nanofluid additives or coating materials on absorber plates. This lets solar energy be turned into heat directly while also driving photocatalytic reactions. This dual-function operation is an example of a new way to build solar thermal and environmental purification

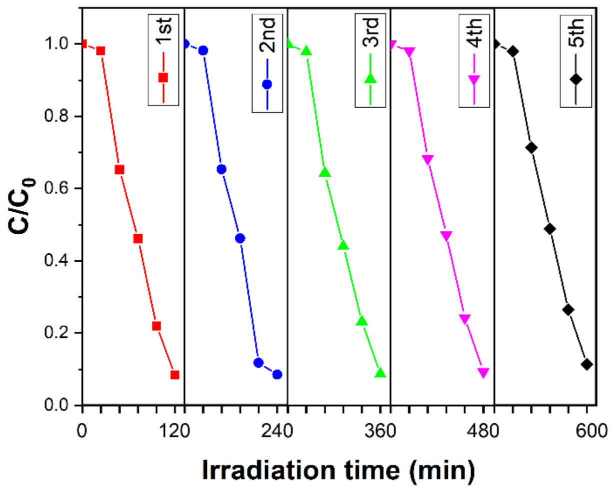

Fig. 8. Reusability experiments for degradation of MB solution using N-CQDs/ZTO nanocomposite.

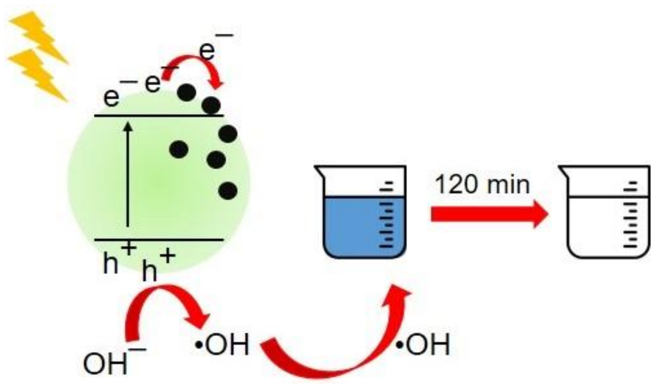

Fig. 9. Possible way that N-CQDs/ZTO nanocomposite can break down MB through photocatalysis.

CC BY

systems in the future.

Evaluation of the efficacy of solar-thermal photocatalysis

Table 1 shows how well the N-CQDs/$Zn_2Ti_3O_8$ nanocomposite works as a photocatalyst at different temperatures that are typical of solar collectors. Strong photothermal synergy is indicated by the observed temperature-dependent increases in degradation efficiency and reaction rate constant. The peak efficiency (98.3 % MB elimination at 70 °C) shows that solar thermal energy efficiently boosts the photocatalytic activity.

CONCLUSION

It has been revealed that the synthesis of the N-CQDs/ZTO nanocomposite is a very effective visible-light photocatalyst. The N-CQDs were produced via hydrothermal reaction utilizing Malva sylvestris extract as the carbon source. PL and DRS spectroscopy revealed that the integration of N-CQDs into the ZTO enhanced visible light absorption and improved charge separation. The results indicated that the N-CQDs/ZTO nanocomposite is capable of degrading organic contaminants. The photocatalytic effectiveness of the nanocomposite was assessed through the degradation of MB solution subjected to visible light for 120 minutes. Using 0.04 g of the nanocomposite at a rate constant of 0.603 min^{-1}, the MB was reduced to 91.7%. We also looked into how the photocatalytic breakdown of MB solution works at different pH levels. We found that alkaline conditions work best for getting the highest level of breakdown. The nanocomposite's photocatalytic effectiveness went up to 97.5% when 1.5 mL of H_2O_2 was added. The reusability tests done over five cycles in a row showed that the nanocomposite that was made is very stable and can be used as a photocatalyst for a long time. The nanocomposite showed a lot of stability over many cycles, which means it could be used in real solar thermal systems. The results show that the N-CQDs/ZTO nanocomposite works well as a photocatalyst for visible light and could be used to collect solar thermal energy because it has a higher photothermal conversion efficiency, stability, and reusability. Adding it to hybrid solar thermal–photocatalytic systems can help make energy production more sustainable and restore the environment. In the future, more research will focus on figuring out how well N-CQDs/ZTO converts solar energy into heat and how to spread it out better in thermal collector fluids so that it works better and stays stable when exposed to real sunlight.

CONFLICT OF INTEREST

The authors declare that there is no conflict of interests regarding the publication of this manuscript.

REFERENCES

1. Hasan MM, Hossain S, Mofijur M, Kabir Z, Badruddin IA, Yunus Khan TM, et al. Harnessing Solar Power: A Review of Photovoltaic Innovations, Solar Thermal Systems, and the Dawn of Energy Storage Solutions. Energies. 2023;16(18):6456.
2. Eze F, Egbo M, Anuta UJ, Ntiriwaa O-BR, Ogola J, Mwabora J. A review on solar water heating technology: Impacts of parameters and techno-economic studies. Bulletin of the National Research Centre. 2024;48(1).
3. Chandran B, Oh J-K, Lee S-W, Um D-Y, Kim S-U, Veeramuthu V, et al. Solar-Driven Sustainability: III–V Semiconductor for Green Energy Production Technologies. Nano-Micro Letters. 2024;16(1).
4. Tian Y, Zhao CY. A review of solar collectors and thermal energy storage in solar thermal applications. Applied Energy. 2013;104:538-553.
5. Wang Z, Changotra R, Dasog M, Singh Selopal G, Yang J, He QS. Carbon quantum dots: Synthesis via hydrothermal processing, doping strategies, integration with photocatalysts, and their application in photocatalytic hydrogen production. Sustainable Materials and Technologies. 2025;44:e01386.
6. Zhang J, Yu S-H. Carbon dots: large-scale synthesis, sensing and bioimaging. Mater Today. 2016;19(7):382-393.
7. Pechnikova NA, Domvri K, Porpodis K, Istomina MS, Iaremenko AV, Yaremenko AV. Carbon Quantum Dots in Biomedical Applications: Advances, Challenges, and Future Prospects. Aggregate. 2024;6(3).
8. Karki D, Thapa YN, Rajchal B, Adhikari R. Recent Advances in the Synthesis of Tailored Carbon Quantum Dots and Their Biomedical Applications. ACS Applied Bio Materials. 2025;8(10):8401-8420.
9. Zhang Y, Yan H, Wang X, Zhang Z, Liu F, Tu S, et al. Highly efficient solar-absorber composite material based on tetrapyridylporphyrin for water evaporation and thermoelectric power generation. RSC Advances. 2022;12(45):28997-29002.
10. He L, He J, Chen E-X, Lin Q. Boosting photothermal conversion through array aggregation of metalloporphyrins in bismuth-based coordination frameworks. Chemical Science. 2024;15(42):17498-17505.
11. Al Sharabati M, Abokwiek R, Al-Othman A, Tawalbeh M, Karaman C, Orooji Y, et al. Biodegradable polymers and their nano-composites for the removal of endocrine-disrupting chemicals (EDCs) from wastewater: A review. Environ Res. 2021;202:111694.
12. Mustafa FS, Oladipo AA. Rapid degradation of anionic azo dye from water using visible light-enabled binary metal-organic framework. Journal of Water Process Engineering. 2024;64:105686.
13. Hassani A, Krishnan S, Scaria J, Eghbali P, Nidheesh PV. Z-scheme photocatalysts for visible-light-driven pollutants degradation: A review on recent advancements. Curr Opin

Solid State Mater Sci. 2021;25(5):100941.
14. Rahbar M, Hosseini-Sarvari M. Natural sunlight-driven photocatalytic mineralization of petrochemical wastewater using ceramic-supported Fe, B co-doped TiO_2/CNT@WO_3 in a flat panel photoreactor. Journal of Water Process Engineering. 2025;77:108328.
15. Wang X, Teo SH, Shamsuddin MR, Wid N. Photocatalytic Degradation of Organic Pollutants and Microplastics Using Ag/TiO_2: Recent Advances in Mechanism, Synthesis and Properties. Water, Air, & Soil Pollution. 2024;236(1).
16. Daghrir R, Drogui P, Robert D. Modified TiO_2 For Environmental Photocatalytic Applications: A Review. Industrial and Engineering Chemistry Research. 2013;52(10):3581-3599.
17. Gao B, Chen GZ, Li Puma G. Carbon nanotubes/titanium dioxide (CNTs/TiO_2) nanocomposites prepared by conventional and novel surfactant wrapping sol–gel methods exhibiting enhanced photocatalytic activity. Applied Catalysis B: Environmental. 2009;89(3-4):503-509.
18. Jabber Al-Saady MAA, Aldujaili NH, Rabeea Banoon S, Al-Abboodi A. Antimicrobial properties of nanoparticles in biofilms. Bionatura. 2022;7(4):1-9.
19. Schneider J, Matsuoka M, Takeuchi M, Zhang J, Horiuchi Y, Anpo M, et al. Understanding TiO_2 Photocatalysis: Mechanisms and Materials. Chem Rev. 2014;114(19):9919-9986.
20. Pelaez M, Nolan NT, Pillai SC, Seery MK, Falaras P, Kontos AG, et al. A review on the visible light active titanium dioxide photocatalysts for environmental applications. Applied Catalysis B: Environmental. 2012;125:331-349.
21. Guo H, Zhang J, Gao J, Liang Z, Li W, Yan H, et al. Carbon quantum dots-modified TiO_2 nanoparticles for antibacterial applications. Chem Phys Lett. 2025;869:142055.
22. Ahmed GHG, Abdelbaky MSM, Garcia-Granda S. Large-scale fabrication of green carbon quantum dots and its nanocomposite with TiO_2 for enhanced photocatalytic oxidation of organic pollutants. Biomass Conversion and Biorefinery. 2024;15(4):5209-5228.
23. Mahmood S, Bi A, Shukla S, Husain S, Prakash J, Chaudhry SA. Synthesis of carbon quantum dots decorated titanium disilicide: a novel hybrid solar-driven photocatalyst for sustainable wastewater treatment. Journal of Materials Chemistry A. 2025;13(37):31781-31801.
24. Benouis K, khane Y, Ahmed T, Albukhaty S, Banoon S. Valorization of diatomaceous earth as a sustainable eco-coagulant for wastewater treatment: optimization by response surface methodology. Egyptian Journal of Chemistry. 2022;0(0):0-0.
25. Prabhakaran PK, Balu S, Sridharan G, Ganapathy D, Sundramoorthy AK. Development of Eco-friendly CQDs/TiO_2 nanocomposite for enhanced photocatalytic degradation of methyl orange dye. Engineering Research Express. 2025;7(1):015002.
26. Najjar M, Sabouri Z, Nasseri MA, Allahresani A, Mostafapour A, Darroudi M. Novel magnetically separable Fe3O4@CQDs photocatalyst: Cytotoxicity effects and photocatalytic performance. J Mater Res. 2025;40(11):1657-1668.
27. Li C, Hu J, Yan H. Study on efficient degradation of sodium lignosulfonate using N-CQDs/$MgIn_2S_4$ composite photocatalyst. Appl Surf Sci. 2025;710:164004.
28. Zhu S, Meng Q, Wang L, Zhang J, Song Y, Jin H, et al. Highly Photoluminescent Carbon Dots for Multicolor Patterning, Sensors, and Bioimaging. Angew Chem Int Ed. 2013;52(14):3953-3957.
29. Rahbar M, Mehrzad M, Behpour M, Mohammadi-Aghdam S, Ashrafi M. S, N co-doped carbon quantum dots/TiO_2 nanocomposite as highly efficient visible light photocatalyst. Nanotechnology. 2019;30(50):505702.
30. Kumar PM, Badrinarayanan S, Sastry M. Nanocrystalline TiO_2 studied by optical, FTIR and X-ray photoelectron spectroscopy: correlation to presence of surface states. Thin Solid Films. 2000;358(1-2):122-130.
31. Shen J, Shang S, Chen X, Wang D, Cai Y. Highly fluorescent N, S-co-doped carbon dots and their potential applications as antioxidants and sensitive probes for Cr (VI) detection. Sensors Actuators B: Chem. 2017;248:92-100.
32. Chen M, Yang F, Hou D, Zheng Y, Liu C, Lin X, et al. Preparation of Multicolor Fluorescent Carbon Dots Based on Catechol and o-Phthalaldehyde. Molecules. 2023;28(14):5303.
33. Manchala S, Nagappagari LR, Muthukonda Venkatakrishnan S, Shanker V. Facile synthesis of noble-metal free polygonal Zn_2TiO_4 nanostructures for highly efficient photocatalytic hydrogen evolution under solar light irradiation. Int J Hydrogen Energy. 2018;43(29):13145-13157.
34. Mebrek A, Alleg S, Benayache S, Benabdeslem M. Preparation and characterization of spinel type Zn_2TiO_4 nanocomposite. Ceram Int. 2018;44(9):10921-10928.
35. Pantoja-Espinoza JC, Domínguez-Arvizu JL, Jiménez-Miramontes JA, Hernández-Majalca BC, Meléndez-Zaragoza MJ, Salinas-Gutiérrez JM, et al. Comparative Study of $Zn_2Ti_3O_8$ and $ZnTiO_3$ Photocatalytic Properties for Hydrogen Production. Catalysts. 2020;10(12):1372.
36. Zhang J, Liu Q, Wang J, He H, Shi F, Xing B, et al. Facile preparation of carbon quantum dots/TiO_2 composites at room temperature with improved visible-light photocatalytic activity. J Alloys Compd. 2021;869:159389.
37. Anandan S, Sathish Kumar P, Pugazhenthiran N, Madhavan J, Maruthamuthu P. Effect of loaded silver nanoparticles on TiO_2 for photocatalytic degradation of Acid Red 88. Sol Energy Mater Sol Cells. 2008;92(8):929-937.
38. Sathish Kumar PS, Sivakumar R, Anandan S, Madhavan J, Maruthamuthu P, Ashokkumar M. Photocatalytic degradation of Acid Red 88 using Au–TiO_2 nanoparticles in aqueous solutions. Water Res. 2008;42(19):4878-4884.
39. Li R, Song X, Huang Y, Fang Y, Jia M, Ma W. Visible-light photocatalytic degradation of azo dyes in water by Ag_3PO_4: An unusual dependency between adsorption and the degradation rate on pH value. J Mol Catal A: Chem. 2016;421:57-65.
40. Alkaim AF, Aljeboree AM, Alrazaq NA, Baqir SJ, Hussein FH, Lilo AJ. Effect of pH on Adsorption and Photocatalytic Degradation Efficiency of Different Catalysts on Removal of Methylene Blue. Asian J Chem. 2014;26(24):8445-8448.
41. Van Doorslaer X, Demeestere K, Heynderickx PM, Van Langenhove H, Dewulf J. UV-A and UV-C induced photolytic and photocatalytic degradation of aqueous ciprofloxacin and moxifloxacin: Reaction kinetics and role of adsorption. Applied Catalysis B: Environmental. 2011;101(3-4):540-547.
42. Rauf MA, Ashraf SS. Fundamental principles and application of heterogeneous photocatalytic degradation of dyes in solution. Chem Eng J. 2009;151(1-3):10-18.
43. Kumar A. A Review on the Factors Affecting the Photocatalytic Degradation of Hazardous Materials. Material Science & Engineering International Journal. 2017;1(3).
44. Rahmani S, Zeynizadeh B, Karami S. Removal of cationic methylene blue dye using magnetic and anionic-cationic modified montmorillonite: kinetic, isotherm and thermodynamic studies. Applied Clay Science. 2020;184:105391.
45. Gaya UI, Abdullah AH. Heterogeneous photocatalytic degradation of organic contaminants over titanium dioxide: A review of fundamentals, progress and problems. Journal of Photochemistry and Photobiology C: Photochemistry Reviews. 2008;9(1):1-12.
46. Wang Y, Hong C-s. Effect of hydrogen peroxide, periodate and persulfate on photocatalysis of 2-chlorobiphenyl in aqueous TiO_2 suspensions. Water Res. 1999;33(9):2031-2036.

cc BY